Agricultural and Forest Meteorology 154–155 (2012) 136–146

Contents lists available at SciVerse ScienceDirect

Agricultural and Forest Meteorology

journal homepage: www.elsevier.com/locate/agrformet

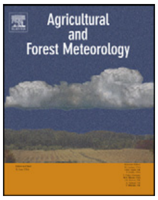

Spatial variability of soil CO_2 efflux linked to soil parameters and ecosystem characteristics in a temperate beech forest

Jérôme Ngao[a,b,*], Daniel Epron[a,b], Nicolas Delpierre[c], Nathalie Bréda[a,b], André Granier[a,b], Bernard Longdoz[a,b]

[a] INRA, UMR 1137 Ecologie et Ecophysiologie Forestières, Centre de Nancy, F-54280 Champenoux, France
[b] Université Henri Poincaré Nancy 1, UMR 1137 Ecologie et Ecophysiologie Forestières, F-54506 Vandoeuvre-les-Nancy Cedex, France
[c] Université Paris-Sud, UMR 8079 Ecologie Systématique et Evolution, Orsay F-91405, France

ARTICLE INFO

Article history:
Received 26 May 2011
Received in revised form 31 October 2011
Accepted 5 November 2011

Keywords:
Soil CO_2 efflux
Spatial variability
Soil C/N ratio
Soil bulk density
Ecosystem respiration

ABSTRACT

The aim of this study was to determine the amplitude and the driving factors of the spatial variability in soil CO_2 efflux in a young European beech forest. Soil CO_2 efflux was measured in 2003 and 2004 in seven beech plots differing in terms of soil type and leaf area index. After eliminating temporal fluctuations due to soil temperature and soil water content, standardized soil CO_2 efflux varied significantly among plots over a large range given the homogeneity of the land cover type. Correlation analyses revealed that this spatial variability could not be explained by root biomass, litter C content, soil C contents, stand basal area or stem density. Conversely, very significant correlations were found with topsoil bulk density, superficial soil C/N ratio, and leaf area index. Multiple regression analysis led to a model relating standardized soil CO_2 efflux to C/N ratio and topsoil bulk density, thus explaining 87% of observed inter-plot spatial variability. This study highlighted the need to consider spatially varying soil factors such as C/N ratio and bulk density when experimental schemes are elaborated to estimate mean soil CO_2 efflux at forest scale.

1. Introduction

Net ecosystem CO_2 efflux (NEE) is measured worldwide by the eddy covariance (EC) technique to quantify terrestrial carbon sequestration and improve our understanding about ecosystem functioning and its response to climate changes (Baldocchi, 2008). NEE is usually partitioned into gross primary productivity (GPP) and total ecosystem CO_2 efflux (R_{ECO}) by assuming R_{ECO} as nighttime NEE measurements and extrapolating them to daytime through empirical relations with temperature and/or soil water content (Desai et al., 2008). However this procedure regularly fails because nighttime EC data do not always match R_{ECO} and/or because EC does not measure fluxes over the same area during nighttime and daytime (e.g. Van Gorsel et al., 2009). Indeed, during relatively stable atmospheric nights, substantial CO_2 amounts can be transported by advection without any transfer through the canopy, and thus without being accounted in R_{ECO} (Aubinet et al., 2005). Despite various corrections, including air friction velocity (u_*) threshold (Ohkubo et al., 2007) and spatial footprint analyses (Rebmann et al., 2005; Göckede et al., 2008), these problems still constitute limiting factors in forest ecosystem studies (Longdoz et al., 2008). Within this context, quantifying and understanding the temporal and spatial variability of soil CO_2 efflux (F_S) can help to support nighttime eddy covariance measurements (i.e. explaining R_{ECO} temporal variability with footprint changes combined with F_S spatial heterogeneities), partition NEE (GPP–R_{ECO}, belowground–aboveground respiration), and close the ecosystem C balance (Ohkubo et al., 2007; Luyssaert et al., 2009). Capturing the high spatial F_S heterogeneity is still a challenge since broad uncertainties remain (Savage and Davidson, 2003; Ohashi and Gyokusen, 2007).

A better understanding of ecosystem carbon fluxes hinges on unraveling abiotic and biotic effects on the major components of R_{ECO} (Valentini et al., 2000), among which F_S accounts for a major share (40–88% of R_{ECO} in forest ecosystems; Granier et al., 2000; Janssens et al., 2001b; Khomik et al., 2006; Luyssaert et al., 2009). Temporal variability of F_S has been shown to be influenced by seasonal fluctuations in both soil temperature and soil water content (Davidson et al., 1998; Epron et al., 1999; Janssens et al., 2003) and by plant photosynthetic activity throughout the seasons (Boone et al., 1998; Högberg et al., 2001; Sampson et al., 2007; Bahn et al., 2009; Marron et al., 2009). In contrast, spatial variability of F_S remains under-researched. Several studies have evaluated the

---

* Corresponding author at: INRA, Clermont Université, Université Blaise Pascal, UMR 547 Physique et Physiologie Intégratives de l'Arbre Fruitier et Forestier, 63100 Clermont-Ferrand, France. Tel.: +33 04 73 62 43 64; fax: +33 04 73 62 44 54.
E-mail addresses: jerome.ngao@clermont.inra.fr (J. Ngao), Daniel.Epron@scbiol.uhp-nancy.fr (D. Epron), nicolas.delpierre@u-psud.fr (N. Delpierre), breda@nancy.inra.fr (N. Bréda), agranier@nancy.inra.fr (A. Granier), longdoz@nancy.inra.fr (B. Longdoz).

0168-1923/$ – see front matter © 2011 Elsevier B.V. All rights reserved.
doi:10.1016/j.agrformet.2011.11.003

Table 1
List of the parameters and abbreviations.

Parameter		Abbreviation	
F_S	Soil CO_2 efflux	NEE	Net ecosystem exchange
T_S	Soil temperature at −10 cm	GPP	Gross primary productivity
θ_S	Volumetric soil water content	R_{ECO}	Ecosystem respiration
T_{SC}	Continuously measured T_S	EC	Eddy covariance
θ_{SC}	Continuously measured θ_S	u_*	Air friction velocity
LAI	Leaf area index	CD	Dystric cambisol
DBH	Diameter at breast height	LCepiS	Luvic epistagnic cambisol
ρ_S	Bulk soil density	LCendoS	Luvic endostagnic cambisol
G	Stand basal area	A_1	Topsoil organo-mineral layer
C/N_{A1}	C-to-N ration of the A_1 layer	CV	Coefficient of variation
R_{10}	Basal soil respiration at 10 °C	SD	Standard deviation
Q_{10}	Coefficient multiplying F_S by 2 for an increase of 10 °C		
a	Parameter of the Gompertz function		
b	Parameter of the Gompertz function		

statistical minimum number of sampling points needed to capture spatial variability and assessed it in relation to either the coefficient of variation, confidence level or semivariance of F_S estimates (Yim et al., 2003; Adachi et al., 2005; Kosugi et al., 2007; Ohashi and Gyokusen, 2007; Knohl et al., 2008). These studies underlined the importance of preliminary studies for defining optimal sampling designs to acquire accurate and reliable field estimates of F_S, but without addressing the determinism of spatial variability.

The few studies that have highlighted spatial determinism have addressed it at various scales, from regional to within-ecosystem scale. They have pinpointed relationships between F_S and soil characteristics (fine root biomass, organic layer thickness, soil C and nutrient contents) or stand structure such as leaf or vegetation area index, mean tree diameter at breast height, canopy closure, leaf litterfall, leaf production, and mean annual precipitation (Xu and Qi, 2001; Reichstein et al., 2003; Søe and Buchmann, 2005; Epron et al., 2006; Khomik et al., 2006; Vincent et al., 2006). An important result from these studies is the temporal evolution of spatial variability (Xu and Qi, 2001; Vincent et al., 2006; Ohashi and Gyokusen, 2007) in relation to factors affecting $F_{S.}$ This underlines the need to identify the potential causes of spatial variability in F_S, especially at within-stand level where footprint modifications mean that F_S variability can induce temporal evolution in eddy covariance-based R_{ECO} measurements (Khomik et al., 2010 and references therein).

The present study aimed at assessing the spatial variability of soil CO_2 efflux in an almost-pure and even-aged European beech (*Fagus sylvatica* L.) stand (Hesse, France). In particular, we addressed the following two questions: (1) at the daily time scale, is the magnitude of spatial variability of F_S comparable at intra-plot scale (ca 40 m^2) and at stand scale (65 ha)? (2) When the dominant influence of soil temperature and soil water content is normalized, what are the main site characteristics that explain the spatial variability of F_S? To answer these questions, soil CO_2 efflux was regularly measured with a portable closed dynamic chamber system via a stratified sampling scheme led over one year. Spatial variability of soil CO_2 efflux was then compared to the main soil and stand characteristics.

2. Materials and methods

2.1. Site characteristics

The study was conducted at the Hesse state forest (48°40′N, 7°04′E, altitude 305 m) in seven plots located in a homogenous 45-year-old beech (*Fagus sylvatica* L.) stand over two consecutive years. Mean annual air temperature was 10.8 °C in 2003 and 9.7 °C in 2004, while annual precipitation was 660 mm in 2003 and 917 mm in 2004. The plot has a gentle slope (<5%, Granier et al., 2000). The soil is more or less severely stagnic cambisol (World Reference Base for Soil Resources) due to an enriched clay layer ranging from 50 to 80 cm depth. A clear shift in soil structure and texture was reported between the E2 (eluviated) and the clay-enriched (clay content ranging from 30 to 40%) layers (Quentin et al., 2001). The spatial variability of the soil properties was described on a 65 ha area, revealing differences in clay layer depth and clay content inducing different soil water dynamics. Three different soils were mapped: the dystric cambisol (CD, no water logging), the luvic epistagnic cambisol (LCepiS, clay content averaging 34% at intermediate 60–80 cm depth), and the luvic endostagnic cambisol (LCendoS, clay content exceeding 37% below 65 cm depth and severe waterlogging periods). The CD and LCepiS soils are covered by an oligo-mull humus while the LCendoS type is covered by a meso-mull humus. Mean pH_{H_2O} and pH_{KCl} values in the 0–10 cm layer reach 4.5 and 3.8, respectively (Quentin et al., 2001). Understory vegetation is sparse. A thinning operation occurred in early 1999 and removed around 25% of stand basal area.

2.2. Soil CO_2 efflux, soil temperature and soil water content

Soil CO_2 efflux (F_S, $\mu mol\, CO_2\, m^{-2}\, s^{-1}$, see Table 1 for the list of the parameters and abbreviations) was measured with a portable closed dynamic chamber (Li 6000-9, Licor, Lincoln, USA; hereafter named “respiration chamber”) connected to an infrared gas analyzer Li-6252 (Licor, Lincoln, USA). The slope of the increase in CO_2 concentration was recorded during 60 s, 15 s after placing the chamber on a collar (Ngao et al., 2006). A foam gasket ring provided an airtight seal between the respiration chamber and the collar. Collars (110 mm diameter, 50 mm height) were inserted into soil (15 mm depth) two weeks before the first measurements, and left inserted throughout the experiment period. There were no measurable (below 0.05 Pa) differences in pressure between the inside and the outside of the chamber, indicating negligible pressure pumping (Longdoz et al., 2000) and no major risks of air leak (Ngao et al., 2006).

Two systems were used for measuring soil temperature at −10 cm depth. The first system (T_S) was a mobile custom-built copper–constantan thermocouple inserted in the soil at −10 cm in the vicinity of the collar selected for the F_S measurement. The second system continuously measured soil temperature (T_{SC}) as the mean of five custom-built copper–constantan thermocouples installed permanently at −10 cm depth at different locations close to the EC tower. Data were acquired every 10 s, and 30 min averages were stored by a CR7 datalogger (Campbell Scientific, Logan, UT, USA).

Similarly, two systems were used for measuring volumetric soil water content. Firstly, during each F_S logging, a ML2x ThetaProbe (Delta-T Devices, Cambridge, UK) was inserted vertically near the selected collar to determine the near-surface soil water content

(θ_S, 0–6 cm). Second, volumetric soil water content at −10 cm depth (θ_{SC}) was continuously measured with four replicates in the vicinity of the EC tower using a time-domain reflectance TRASE system (SoilMoisture Equipment Corp., Santa Barbara, CA, USA). Site-specific calibration was used for each soil layer. All subsequent analyses were conducted at the daily time-scale, by computing daily means of soil temperature and soil water content.

2.3. Soil CO_2 efflux sampling strategy

The sampling scheme was developed based on the results of two preliminary studies held prior to the main campaign. The first study consisted of a series of F_S measurements performed on 12 collars installed close to the EC system tower during 24 h in June of 2003, i.e. when high photosynthetic activity was expected (Granier et al., 2000). There were no significant variations in F_S averaged across the 12 collars over the 24 h timespan, while T_S varied less than 4 °C during the same timespan. This 24-h study was repeated in July of 2004, giving similar outcomes. It was concluded that at plot level, mean F_S does not vary significantly at the daytime timescale (if this temporal variation exists at the collar level, it should be smoothed when spatial averaging is performed). This allowed us to measure F_S throughout daytime during the main measurement campaign, when daily T_S variations were lower than 4 °C. This T_S range was observed for 29 of the 31 days constituting the complete campaign. During two days in 2004, the daily range was 4.5–5 °C in two plots but the measurements were included in the data set as the coefficient of variation remained in the same range as (or even lower than) the other plots. During the second preliminary study, F_S was measured on 42 collars placed on a grid (30 m × 140 m, 10 m mesh) and on 28 collars placed at 1 m intervals along 4 parallel transects (transects 2 m apart). The semivariances (data not shown) obtained in both cases did not show any variation with distance between measurements points. Thus, in the following, two measurements of F_S at least 1 m apart will be considered as spatially independent.

The sampling scheme for the main F_S survey was designed to cover the largest range for two of the parameters that are likely to drive spatial F_S variations at stand level, i.e. soil type, which influences relative soil water content and rooting distribution, and leaf area index (LAI, Granier et al., 2000), which affects root biomass and soil C content. Seven plots (40 m^2) were chosen across the stand based on these criteria (Table 2 and Fig. 1). Within each plot, 12 PVC collars were inserted in soil following two crossing transects. Building on the preliminary studies (see above), the distance between two collars was set to 1 m and the plots are spaced from 20 m to 700 m apart. At each measurement day, F_S was measured on the 12 collars of the 7 plots. Both T_S and θ_V were measured concurrently in the close vicinity of the F_S collars. Data were averaged by plot, assuming that the surface covered by the collar transects is representative of the local soil and stand characteristics. The overall measurement survey took place between 7:30 (GMT) and 16:00 every two–three weeks, over 18 months.

Table 2
Main characteristics of the plots studied. The plots were chosen based on soil type: CD type (no water retention, no differentiated clay layer), LCepiS type (clay content averaging 34% in intermediate 60–80 cm depth), and LCendoS type (clay content exceeding 37% below 65 cm depth and water saturation events during winter). Tree age (years), tree height (m), soil available water capacity (AWC, mm) and leaf area index (LAI, $m^2\ m^{-2}$) are also given. The AWC is the quantity of water that plants can extract from the soil. It is defined as the water amount comprised between the field capacity and the permanent welting point integrated all along the root profile.

Plot	Soil type	Age (2004)	Height (m)	AWC (mm)	LAI (2004)
#110	LCepiS	40	16.2	107	6.9
#85	LCendoS	40	14.0	87	5.6
#72	LCendoS	40	16.3	84	7.2
#73	LCepiS	40	17.2	121	5.8
#75	CD	40	19.3	124	8.1
#87	LCendoS	40	14.4	93	4
#122	LCepiS	60	>22.5	134	6.9

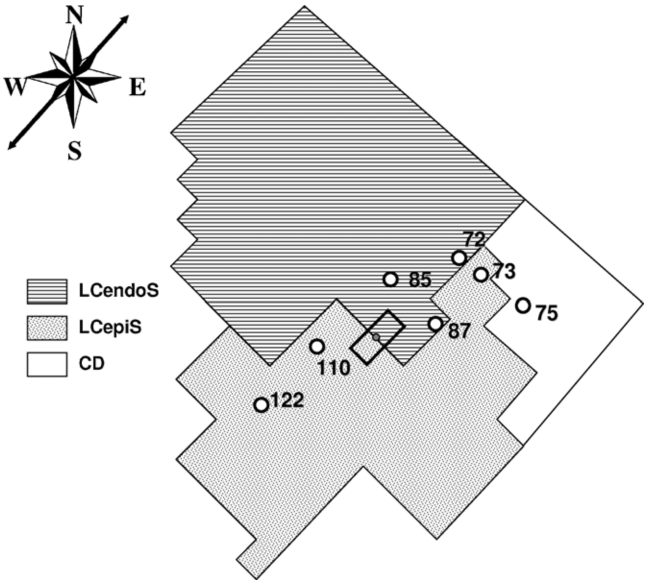

Fig. 1. Schematic map of the site showing the different plot locations on the three different soil types (LCendoS: highest clay content, LCepiS: intermediate clay content, CD: lowest clay content). The thick arrow indicates the dominant wind direction. The grey dot at the center of the study site represents the eddy flux tower. Adapted from Bouriaud et al. (2003).

2.4. Stand and soil parameters

LAI ($m^2\ m^{-2}$) at the center of each plot was determined in mid-summer by two operators using two inter-calibrated LAI2000 (Licor, Lincoln, USA) with a 180° restrictor view, one below canopy and the other on top of the EC tower. Diameter at breast height (DBH, m) was measured on all trees inside a 7 m-diameter area centered on the collar transects crossover on all plots at the end of 2004. Basal area (G) and tree density of each plot were then calculated.

For each plot, six soil cores (15 cm depth, 8 cm diameter) were sampled at the end of 2004. Leaf and woody litter was separated from bulk soil. Then, the topsoil organo-mineral layer (hereafter coded "A_1 layer") was gently isolated from the mineral soil beneath (hereafter named "mineral soil"), according to a clear and sharp visual transition between the highly organic black-colored upper part and the bright brown-colored lower part. The living and dead roots were retrieved from the leaf litter and the A_1 layer, carefully washed with deionized water, and kept at 4 °C prior to drying. The remaining mineral soil was sieved at 2-mm mesh size, and most of the roots were manually retrieved as described above. Remaining aggregates were partly dissolved in distilled water for 24 h and sieved (2- and 1-mm mesh size) to retrieve the remaining roots. Leaf litter, roots and bulk soil (A_1 and mineral layer) were dried at 50 °C for subsequent carbon and nitrogen content determination on an NCS2500 elemental analyzer (CE Instrument ThermoQuest, Italy). Concurrently, topsoil bulk density (ρ_S, in g cm^{-3}) was estimated for each plot by sampling 9 soil cores with steel cylinders (5 cm depth, 8 cm diameter) following the collar transects. The soil cores were dried for five days at 105 °C, and then weighed. All soil cores were taken around 1.5 m next to the collar transects, avoiding the compaction zone resulting from the repeated operator passage for the F_S measurements.

Table 3
Parameters (asymptotic standard deviation in parentheses) of Eq. (1) (R_{10i}, Q_{10i}, a_i and b_i) fitted on soil CO_2 efflux, temperature and water content data per plot. Mean annual F_S (kg C m^{-2} y^{-1}) ± standard deviation was calculated by summing the daily F_S computed by applying Eq. (1) (see text for method details). The coefficient of determination (R^2) and root mean square error (RMSE) are also given.

Plot	R_{10i}	Q_{10i}	a_i	b_i	R^2	RMSE	Annual F_S
#110	1.63 (0.11)	2.49 (0.34)	0.97 (0.65)	25.3 (11.35)	0.68	0.42	0.6 (0.03)
#85	2.37 (0.18)	2.73 (0.37)	1.13 (0.37)	17.52 (6.06)	0.75	0.5	0.79 (0.06)
#72	1.44 (0.14)	2.35 (0.47)	1.17 (0.65)	21.97 (10.78)	0.53	0.46	0.51 (0.05)
#73	1.62 (0.13)	2.4 (0.43)	1.34 (0.63)	25.54 (11.63)	0.61	0.41	0.58 (0.03)
#75	1.46 (0.14)	2.54 (0.45)	0.27 (0.49)	15.7 (10.20)	0.66	0.38	0.52 (0.05)
#87	2.1 (0.16)	2.45 (0.35)	0.25 (0.32)	14.74 (6.13)	0.72	0.49	0.73 (0.05)
#122	1.78 (0.17)	2.89 (0.51)	0.89 (0.44)	19.56 (9.04)	0.68	0.47	0.63 (0.07)

2.5. Data analysis

One F_S (in μmol CO_2 m^{-2} s^{-1}), T_S and θ_S value was obtained for each of the seven plots and for each measurement day (F_{Si}, T_{Si} and θ_{Si} with a subscript *i* referring to the plot number) by averaging the data from the twelve collars within each plot. Seasonal variations of these values were co-related by a relationship including the product of a Q_{10} function (for temperature dependency) and a Gompertz function (for soil water content dependency, Janssens et al., 2001a):

$$F_{Si} = R_{10i} Q_{10i}^{((T_{Si}-10)/10)} e^{-e(a_i - b_i \theta_{Si})} \quad (1)$$

where R_{10i} is basal respiration at 10 °C, Q_{10i} is the parameter reflecting the temperature sensitivity of F_S, and a_i and b_i are the parameters of the simplified Gompertz function, which allows a positive influence of θ_S on F_S at low water content (Janssens et al., 2001a). A limiting effect for higher θ_S values was not included in Eq. (1) as Epron et al. (1999) did not find any decrease in F_S related to a rise in soil water content at the same site. Eq. (1) was fitted on a temporal series of daily-averaged F_S, T_S and θ_S values (at least 26 dates per adjustment) for each plot.

Determination of daily F_S value (g C m^{-2} d^{-1}) and temporal integrations to annual F_{Si} (kg C m^{-2} y^{-1}) were performed for each plot. In a first stage, one linear relationship per plot *i* was established between the daily mean T_{Si} values and the corresponding daily mean values of continuously measured soil temperature (T_{SC}). The same procedure was performed between daily mean θ_{Si} and the daily mean values of continuously measured soil water content (θ_{SC}), leading to a set of two linear equations per plot (one for temperature, the other for soil water content). All linear relationships had R^2 values ranging from 0.91 to 0.97 (data not shown). Then, the evolution in daily means of T_{Si} and θ_{Si} for each plot were reconstructed from the T_{SC} and θ_{SC} mean values as inputs of the different linear relationships. Finally, these reconstructed T_{Si} and θ_{Si} values were employed in Eq. (1) to compute a daily simulated F_{Si} (in g C m^{-2} d^{-1}). Annual soil CO_2 efflux (kg C m^{-2} y^{-1}) was computed for 2004 as the sum of the simulated daily F_{Si}. An annual sum could not be computed for 2003 as the F_S measurements started in August 2003.

2.6. Statistical analyses

The amplitude of the spatial variability of F_S at stand scale was characterized for each measurement day by calculating the coefficient of variation (CV), i.e. the ratio between the standard deviation (SD) and the mean value, using data from all the collars of the study site. Intra-plot variability was cross-analyzed against whole-stand variability to assess the impact of the sampling scheme (choice in the number of collar by plot, spatial disposition and extent of the plots). This cross-analysis was performed for each measurement date by comparing the observed SD on 12 collars within a plot (SD_{meas}) to a distribution of simulated SD values calculated (SD_{sim}) at stand level. The SD_{sim} were obtained from 12 F_S measurements randomly chosen (i.e. assuming no spatial influence of collar location) from the total number available by bootstrapping (Matlab 7, The MathWorks Inc., USA). The SD_{sim} distribution was constructed from 1000 SD_{sim} values. The fraction of SD_{sim} being higher than the actual SD_{meas} was calculated (*isup* index). An *isup* index either higher than 0.95 or lower than 0.05 reflects a plot with, respectively, a significantly lower or significantly higher spatial variability than the entire site, and thus the F_{Si} of the plot could be considered as specific and influenced by its spatial location.

Two-way ANOVA was performed to test the effects of plot, measurement day and their interactions on mean F_S, T_S and θ_S ($n = 12$; SAS 8.1, SAS Institute Inc., USA). One-way ANOVA was performed to test the effects of plot on soil density and on the C and N contents of either leaf litter, roots, mineral layer or A_1 layer. Eq. (1) was fitted to the data by least squares non-linear regression analyses on each plot data set for the whole time series, giving one parameter set (R_{10}, Q_{10}, a, b) per plot. Pairwise comparisons were run on each model parameter by calculating a *t* statistic which was then tested at the significance level of $p = 0.002$. This p value corresponds to the Bonferroni correction defined as $p = \alpha/n_t$ where n_t is the number of independent pairwise tests among seven plots and α is significance level ($n_t = 21$, $\alpha = 0.05$; Williams, 1993). The SDs of plot annual F_S were estimated by drawing 1000 sets of Eq. (1) parameters, with each parameter drawn from normal distributions characterized by their fitted means and SDs (Table 3). Each parameter set drawn was used to re-compute daily F_S using Eq. (1) with the reconstructed daily means for T_{Si} and θ_{Vi} (see Section 2.5), which were summed to give 1000 values for annual F_S. Linear correlation analyses and a stepwise regression analysis were performed to correlate R_{10i} with different stand and soil parameters. For all ANOVAs and linear regressions, significance level was set at $p = 0.05$.

3. Results

3.1. Soil CO_2 efflux, soil temperature and soil water content

F_{Si} showed a general seasonal pattern common to all plots, varying from 0.24 ± 0.10 μmol CO_2 m^{-2} s^{-1} (mean ± 95% confidence interval) to 4.1 ± 0.94 μmol CO_2 m^{-2} s^{-1} (Fig. 2a). There were significant differences in mean F_{Si} among the plots for each date (except two), with a significant date × plot interaction.

Both T_{Si} and θ_{Si} also showed very similar seasonal patterns in all the plots (Fig. 2b and c). The differences in T_{Si}, even when significant, were never greater than 2 °C across plots. We found significant differences in θ_{Si} within a maximal range of 0.1 m^3 m^{-3} among plots. No hierarchy according to soil type in the upper layer was found.

The spatial CV of F_S varied throughout the measurement period, ranging from 9% to 62% among the plot (Fig. 3a). The CV of T_S and θ_S varied from 1% to 44% (Fig. 3b) and from 0.2% to 60%, respectively

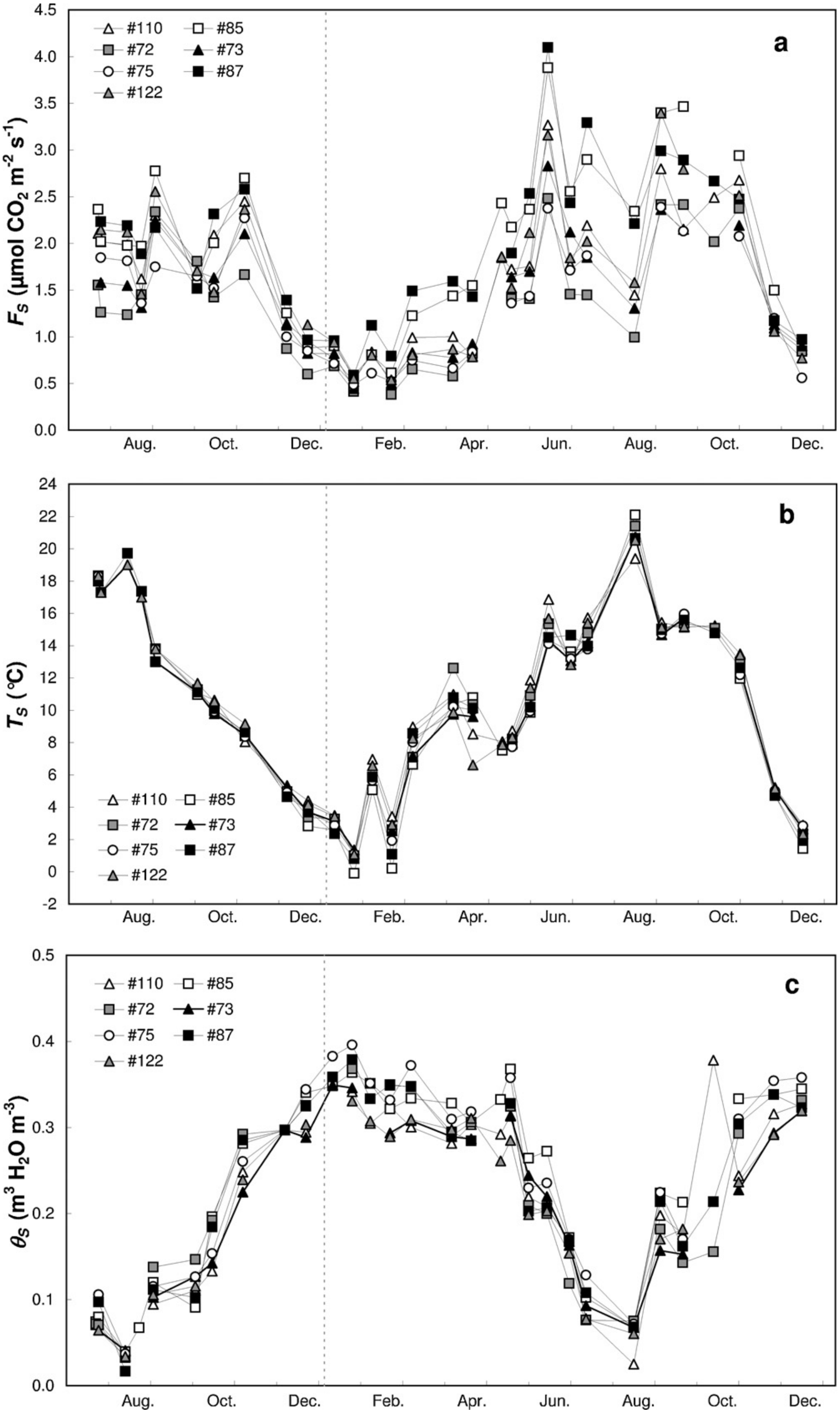

Fig. 2. Temporal variations of mean soil CO$_2$ efflux F_S (a), local soil temperature at −10 cm T_S (b) and local soil water content in the 0–6 cm layer θ_S (c) in each plot ($n = 12$). The vertical broken line indicates the limit year between the 2003 and 2004.

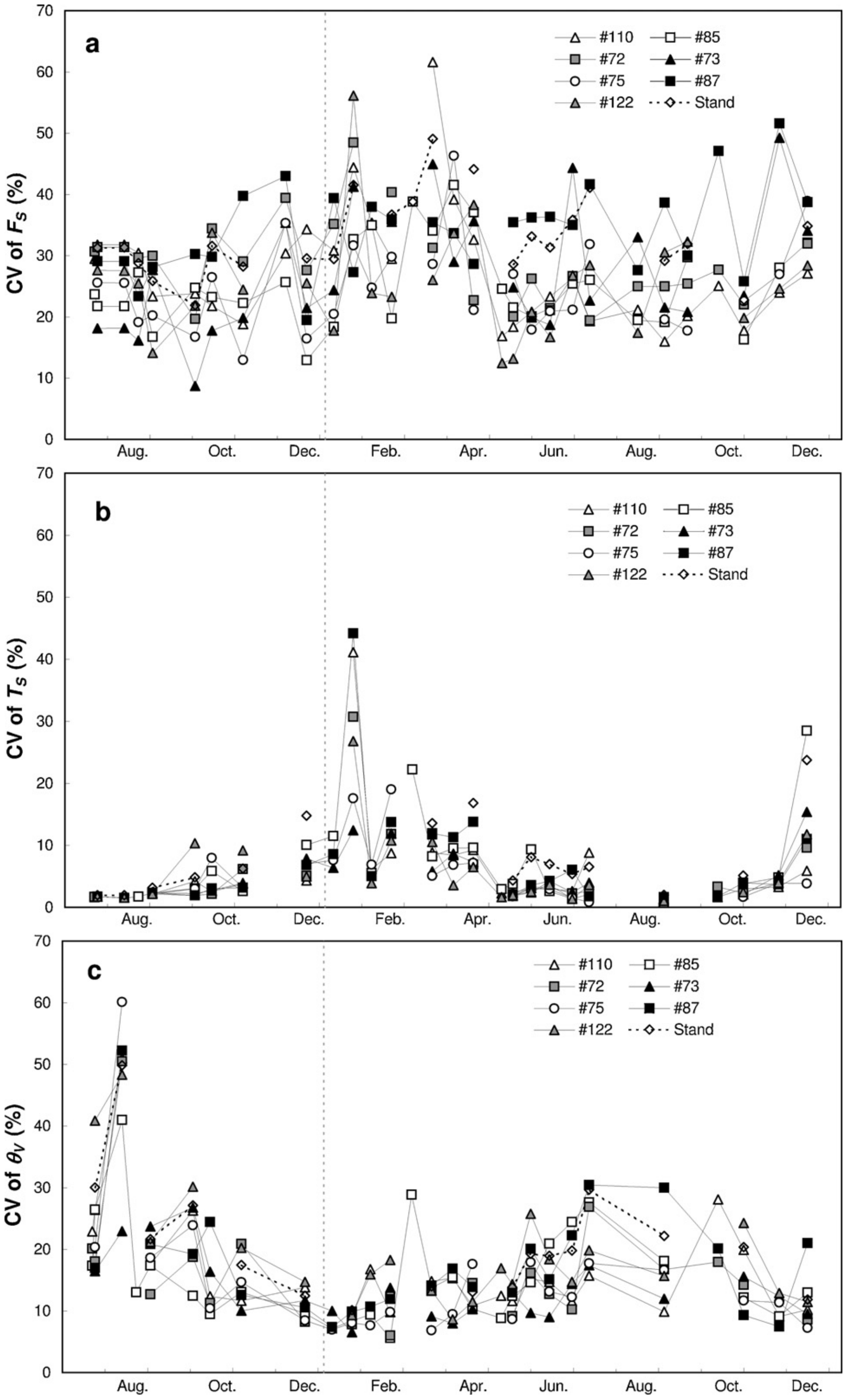

Fig. 3. Temporal variations in coefficient of variation (CV) of soil CO_2 efflux F_S (a), local soil temperature at −10 cm T_S (b) and local soil water content in the 0–6 cm layer θ_S (c) in each plot ($n = 12$). The stand-scale CV is also given and calculated when all the plots were measured. The vertical broken line indicates the limit year between the 2003 and 2004.

(Fig. 3c). When considering all the plots, *isup* index was higher than 50% for around 68% of the measurement days, while *isup* index was above 95% for 15% of the measurement days. These results indicate a significantly smaller spatial variability of F_S at plot scale than at stand scale during these days. The occurrence of 95%-*isup* indices was higher for the plots #73 and #75 (26% and 29% of the measurement days throughout the year) than for the other plots (3–12% of the measurement days). This test showed that the main share of the F_S measurements were statistically less variable at plot scale than at entire stand scale.

Table 4
Means (±standard deviation when available) of stand and soil variables determined within a 7-m-diameter area centered on the collar transects: tree density (n, stem ha^{-1}); basal area (G, m^2 ha^{-1}) calculated on all trees or only for beech (in parentheses); leaf area index in 2004 (LAI, m^2 m^{-2}); soil bulk density of the 0–5 cm layer (ρ_S, g cm^{-3}); C-to-N ratio of the A$_1$ layer (C/N$_{A1}$); mean C and N contents (kg m^{-2}) determined in the different pools in the 0–15 cm soil layer (leaf litter, roots, bulk mineral soil). Total mean C and N contents were calculated directly by summing the C and N contents of different pools by each core. The root pool integrated both living and dead roots.

Plot	n	G	LAI	ρ_S	C/N$_{A1}$	C				N			
						Litter	Roots	Soil	Total	Litter	Roots	Soil	Total
#110	7016	47.5 (44.0)	6.9	0.8 (0.1)	10.9 (0.8)	50 (21)	11 (7)	245 (31)	413 (56)	1.2 (0.5)	0.2 (0.1)	29 (3.6)	38 (5.2)
#85	7535	35.7 (22.8)	5.6	0.7 (0.3)	11.7 (0.8)	17 (9)	13 (12)	260 (23)	403 (51)	0.3 (0.2)	0.2 (0.2)	24.8 (2.2)	33 (4.3)
#72	4158	44.3 (30.0)	7.2	0.9 (0.1)	10.2 (1.2)	33 (14)	08 (07)	265 (51)	379 (65)	0.6 (0.3)	0.2 (0.1)	23.8 (4.5)	31 (5.8)
#73	3898	30 (30)	5.8	0.8 (0.1)	9.6 (0.2)	41 (19)	16 (2.3)	227 (20)	361 (39)	1.1 (0.5)	0.2 (0.3)	26.0 (2.3)	33 (2.8)
#75	3638	45.3 (37.3)	8.1	0.9 (0.2)	10.1 (0.8)	50 (19)	10 (12)	321 (44)	440 (58)	1.3 (0.5)	0.1 (0.1)	26.9 (3.7)	33 (4.7)
#87	3638	53.9 (3.2)	4	0.8 (0.01)	11.7 (1.0)	33 (15)	7 (6)	340 (49)	521 (70)	0.8 (0.4)	0.1 (0.1)	30.8 (4.4)	43 (6.0)
#122	7276	48.7 (34.6)	6.9	0.9 (0.1)	11.2 (1.1)	42 (20)	18 (23)	312 (29)	510 (47)	1 (0.5)	0.3 (0.4)	31.3 (2.9)	42 (3.5)

3.2. Factors influencing temporal variations of soil CO$_2$ efflux

The fitted parameters of Eq. (1) on individual plots are summarized in Table 3. The multiple model parameter pairwise tests showed that the R_{10i} parameters in plots #85 and #87 were significantly higher than in the other plots, while the Q_{10i}, a_i and b_i parameters were not (Table 3). Residual F_S were unbiased when plotted against either T_S or θ_S (data not shown). Temporal integration to annual F_S resulted in large spatial differences ranging from 0.51 ± 0.05 kg C m^{-2} y^{-1} (plot #72) to 0.79 ± 0.06 kg C m^{-2} y^{-1} (plot #85, Table 3).

3.3. Spatial variation of soil characteristics

We found significant among-plot differences in soil parameters (Table 4). One-way ANOVA showed significant differences in topsoil density (ρ_S) and in C and N contents of the A$_1$ layer, leaf litter and mineral soil. In contrast, no significant differences were found in either living, dead or total root biomass. The C/N ratio of the A$_1$ layer (C/N$_{A1}$) ranged from 9.5 to 11.8.

3.4. Relationships between soil CO$_2$ efflux and plot characteristics

The correlation analyses revealed that R_{10i} was significantly and linearly correlated to ρ_S ($r = -0.81$, $p = 0.0056$; Fig. 4a), C/N$_{A1}$ ($r = 0.86$, $p = 0.0020$; Fig. 4b) and LAI ($r = -0.83$, $p = 0.0035$; Fig. 4c). LAI and C/N$_{A1}$ were negatively correlated ($r = -0.79$, $p = 0.01$). R_{10i} was not correlated with the C or N contents of bulk soil, A$_1$ layer, litter, or roots. We then performed a stepwise regression with R_{10i} as dependent variable and ρ_S, LAI and C/N$_{A1}$ as independent variables. This stepwise procedure tested combinations of two of these three parameters and the different parameter integrations into the model. It appeared that adding LAI did not significantly improve the regression, which can be written:

$$R_{10i} = -1.472\rho_{Si} + 0.192\,\mathrm{C/N}_{A1i} \quad (2)$$

where the subscript i refers to the plot. This relationship was found to explain a very large share of the variability of R_{10i} ($R^2 = 0.87$, $p = 0.0022$).

4. Discussion

4.1. Intra-plot vs. stand-scale spatial variability of F_S measurements

The resulting number of collars per plot made it possible to obtain mean values that integrate the local spatial variability with a CV ranging from 9% to 62% (Fig. 3), i.e. comparable to other studies with similar or greater numbers of measurements (Yim et al., 2003; Adachi et al., 2005; Epron et al., 2006; Khomik et al., 2006; Kosugi et al., 2007). Moreover, comparing simulated distributions of stand-scale SD with measured intra-plot-scale SD showed that for a certain number of measurement days, variability observed at intra-plot scale was lower than that of the one at the whole stand scale. For a greater number of measurement days, intra-plot

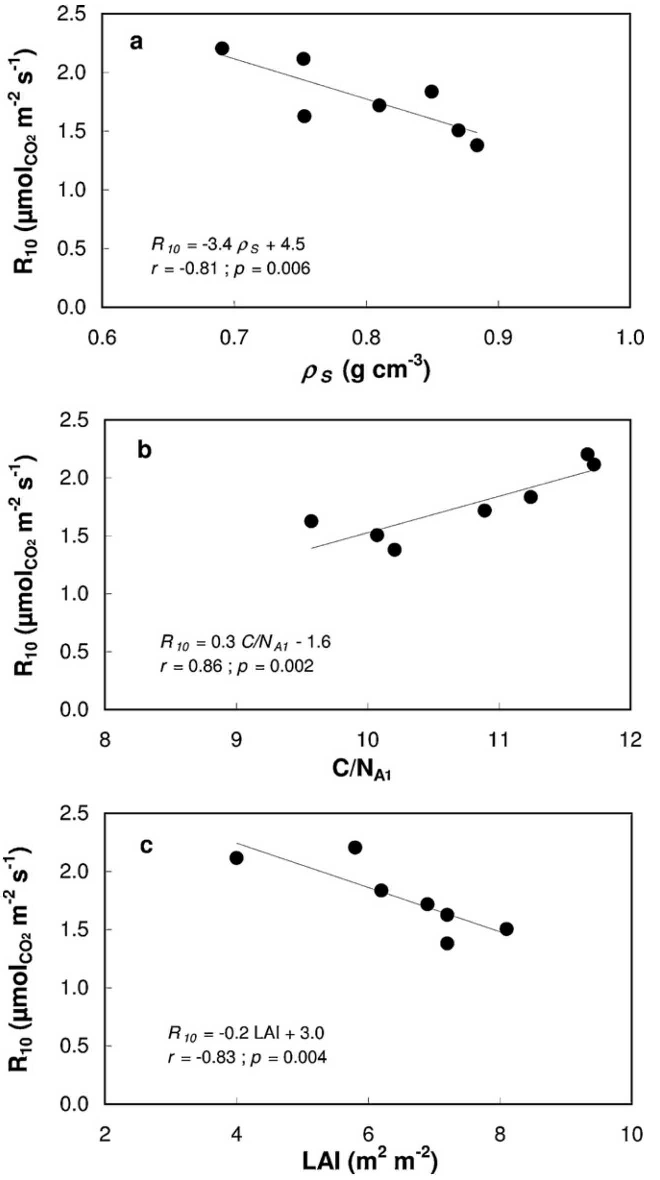

Fig. 4. Relationships between the basal soil CO$_2$ efflux at 10 °C (R_{10i}) and topsoil bulk density (ρ_S, a), C/N ratio of the A$_1$ layer (C/N$_{A1}$, b) and LAI (c). Linear correlation coefficients (r) and the p values are given for each relationship.

variability was not significantly different to the variability observed at whole-stand scale. In addition, the SD values of our R_{10} parameters (Table 3) were in very good agreement with those obtained by Rodeghiero and Cescatti (2008) with 12 collars in three different sites. Knohl et al. (2008) showed in an old unmanaged forest that it takes about 8 sampling locations to achieve a precision in the soil respiration estimate of 20% of the full population mean at a 95% confidence level. It appears that the heterogeneity of F_S observed in the Hesse forest is consistent with that of other studies.

4.2. Seasonal and spatial variations of F_S

Eq. (1) explained a large share ($R^2 > 53\%$) of the seasonal variations in F_S (Table 3). The Q_{10} values were lower than previously reported by Epron et al. (1999) for the same forest, but remained within the range of other published reports for temperate forests (see the listed values reported by Bahn et al., 2010). Integrating measurements made in 2003 during the summer drought made it possible to expand the θ_S range and thus to underline the effect of θ_S on F_S (Fig. 2). Adding θ_S greatly improved the performance of the F_S model, as it allowed to explain 23% more variance than when only temperature was considered as an independent variable. This confirmed that the inhibitory role of low soil moisture, that is well described for Mediterranean ecosystems (Reichstein et al., 2002; Rey et al., 2002; Curiel Yuste et al., 2003) and tropical ecosystems (Epron et al., 2004b), can have equally large impacts in temperate forests (Epron et al., 2004a; Vincent et al., 2006). Modeling of the effect of soil water on F_S could be improved by using a more functional soil water parameter such as water-filled pore space (Franzluebbers, 1999). The remaining variability unexplained by Eq. (1) could be attributed to seasonal variations of both root and soil microbial biomass (Epron et al., 2001; Ruehr and Buchmann, 2010).

We found significant among-plot differences in R_{10i} values. The range of our R_{10i} values was consistent with the values reported in other studies on temperate ecosystems (Epron et al., 1999; Longdoz et al., 2000; Epron et al., 2001; Janssens and Pilegaard, 2003; Subke et al., 2003; Curiel Yuste et al., 2005; Rodeghiero and Cescatti, 2008; Sampson et al., 2007; Vincent et al., 2006; Ngao et al., 2007; Chemidlin Prévost-Bouré et al., 2010). Unfortunately, soil basal respiration rate (like R_{10}) values are not as frequently reported in the literature as Q_{10} data (Davidson et al., 2006), whereas Bahn et al. (2010) showed that the basal respiration of a given site at mean annual soil temperature (R_{MAT}) is actually sufficient to predict annual total soil CO_2 efflux whatever the vegetation type or biomes, in non-water-limited sites. At Hesse, mean annual soil temperature was 9.9 °C for both 2003 and 2004, and thus the R_{10} values in the present study are very close to R_{MAT} (data not shown) and consistent with the values published by Bahn et al. (2010) for beech stands.

4.3. Spatial variation of plot characteristics and links to model parameters

Very few studies have employed a stratified sampling scheme, i.e. organizing the measurement points into independent subpopulations, to identify the ecosystem parameters potentially influencing the spatial variability of F_S (Xu and Qi, 2001; Tang and Baldocchi, 2005; Saiz et al., 2006; Epron et al., 2006; Vincent et al., 2006). Here, the full set of measurement points were distributed among different combinations of LAI classes and soil types, making it possible to observe the spatial variability of R_{10i} and its relation to spatial variability of topsoil ρ_S and C/N_{A1} (Eq. (2)). There have been only rare attempts to relate R_{10} variability to environmental factors. Vincent et al. (2006) proposed a similar approach to ours through an empirical model linking temporal variability of F_S with soil temperature and soil water content in 9 plots in a mixed deciduous forest. In their study, the R_{10} parameter was positively related to plot basal area and to soil pH measured either in water or KCl. The optimal soil water content parameter was positively correlated to bulk density and topsoil N content. At a much larger scale, Reichstein et al. (2003) described an empirical model fitted to data from 17 forest and shrubland sites in Europe and North America. They showed that basal rate of F_S (equivalent to our R_{10} parameter) was positively and linearly dependent on site peak site LAI, implying a relationship with site productivity in agreement with Janssens et al. (2001b). The negative relationship between R_{10} with high LAI in our study could be attributed to heterogeneity of the water balance, through both higher rainfall interception and higher stand evapotranspiration (Bréda, 1999; Granier et al., 1999). Throughfall, i.e. the fraction of rainfall reaching the upper litter and soil, is then more limited and more variable for higher LAI, especially for small rainfall events occurring during the summer. Then the upper litter and soil layers remain drier with limited re-watering than for lower LAI. In consequence, soil CO_2 efflux is also limited, which could explain the negative relationship we observed. This hypothesis could also be supported by a correlation between plot LAI and the CV of θ_V calculated at the plot scale, which has been found higher during summer 2004 than the other seasons (data not shown). Such relationship between LAI with mean θ_V or CV of mean soil temperature was not found. In addition, we found no relationships between R_{10} and plant parameters such as fine root biomass or mean DBH, in contrast to Søe and Buchmann (2005) in old mature broad-leaved forest (tree age in a large range up to 250 years). Saiz et al. (2006) showed in a Sitka spruce chronosequence (tree age from 10 to 47 years) that a decrease in root respiration can be explained by a decrease in fine root biomass over a chronosequence. The lack of relationships with root biomass could be attributed to the narrower tree age range at Hesse (40–60 years, Table 4). It thus appears that the determinants of R_{10} vary among studies, implying site-dependent intrinsic characteristics that present a relatively large range of variation and which might influence particular processes driving F_S.

At the Hesse site, the variations in topsoil density probably result from influences of both forest management and variability of topsoil texture (loam/clay ratio), but very few studies are available on this topic for forest soils (Mariani et al., 2006). At Hesse, one source of higher topsoil bulk density may be compaction following thinning and regeneration operations. Higher topsoil bulk density potentially influences soil CO_2 efflux by reducing topsoil porosity and thus decreasing both O_2 and CO_2 diffusivity, but no consensus emerged from the recent review by Beylich et al. (2010). Moreover, the plots with the lowest ρ_S also exhibited substantially higher earthworm turricules, which could indicate greater earthworm activity within the unsaturated zone (0–35 cm), thus enhancing gas diffusion. These two arguments (reduction of O_2 and CO_2 diffusion, earthworm activity) may potentially combine to explain the negative relationship between R_{10i} and ρ_S found in this study.

A positive relationship was found between R_{10i} and C/N_{A1} (Fig. 4). Khomik et al. (2006) reported a spatially negative relationship between F_S and the C/N ratio of a shallow layer (i.e. the LFH litter layer), in agreement with Taylor et al. (1989) and Longdoz et al. (2000). Indeed, numerous studies have shown that higher-quality litter (often seen as higher N-content litter, i.e. a lower C/N ratio) decomposes faster, resulting in enhanced microbial activity and increased litter mass loss (Melillo et al., 1982; Norby et al., 2001; Vesterdal et al., 2008). However, this negative relationship was generally established among different sites and species, and occurred for C/N ratio measured in foliar decomposing litter with values evolving in much higher ranges than the values found here

(9.5–11.8) that were measured in the A_1 layer. Leuschner et al. (2006) observed a slight negative relationship between stand leaf mass and topsoil C/N for different European beech stands across a gradient of soil acidity and precipitations and with a higher range of C/N (15–30) than in our study. Vesterdal et al. (2008) and d'Annunzio et al. (2008) measured C/N ratio values in the top mineral soil of European beech plots, and their reported values were closer to ours (C/N from 13 to 22). d'Annunzio et al. (2008) also showed that when the N content of top mineral soil is relatively high and decomposers are sufficiently supplied with labile carbon from the humus, litter decomposes more completely than when the decomposers are carbon-limited. Consequently, our positive relationship between R_{10i} and the C/N_{A1} probably reflects better C consumption efficiency (rather than an effect of C supply) with increasing C/N ratios (and consequently higher R_{10} levels) under non-limiting N conditions.

Our study found no significant difference in Q_{10} among plots, contrary to Xu and Qi (2001). There is a consensus that Q_{10} is higher for rhizospheric respiration than for heterotrophic decomposition (Boone et al., 1998; Epron et al., 2001; Lavigne et al., 2004). Consequently, the relative contributions of both F_S components (autotrophic and heterotrophic soil respiration) potentially influence the Q_{10} of F_S. Ngao et al. (2007) partitioned F_S in the Hesse forest at two plots close to the stand studied here but with contrasted species composition and beech tree age. Despite the low number of replicates, they showed that the site with the largest autotrophic contribution also gave a higher Q_{10} value. Following these results, which need to be verified with a higher number of replicates, the across-plot Q_{10} found in this study would reflect a fairly constant partitioning of rhizospheric and heterotrophic contributions to F_S, in accordance with the relative spatially homogeneous root biomass of our site (Table 4). However, the R_{10} and Q_{10} estimates did not integrate seasonal changes in living root biomass or soil microbial biomass, the activity of which could likely be influenced by spatial variation of T_S and/or θ_V, as hypothesized above. Root and soil microbial biomass dynamics, which are not available for our study, should be more taken into account for better modeling both temporal and spatial variations of F_S.

4.4. Annual F_S and comparison to R_{ECO}

In 2004, the annual F_S varied among plots from $0.51 \pm 0.05\,\mathrm{kg\,C\,m^{-2}\,y^{-1}}$ to $0.79 \pm 0.6\,\mathrm{kg\,C\,m^{-2}\,y^{-1}}$ (Table 3), giving a very large relative range of 55%. These values covered the range for intermediate (10–40 years) temperate forests as reviewed by Subke et al. (2006) and more particularly for European *Fagus sylvatica* forests as reviewed by Bahn et al. (2010), thus revealing that intra-stand spatial variability of annual F_S could be as large as the inter-site spatial variability of R_{ECO} (Granier et al., 2007).

From 1996 to 2007, the R_{ECO} for the Hesse site varied from $0.79\,\mathrm{kg\,C\,m^{-2}\,y^{-1}}$ to $1.29\,\mathrm{kg\,C\,m^{-2}\,y^{-1}}$ (Granier et al., 2008). The spatial variability of F_S ($0.28\,\mathrm{kg\,C\,m^{-2}\,y^{-1}}$) is thus not negligible compared to the inter-annual variations in R_{ECO} (up to $0.49\,\mathrm{kg\,C\,m^{-2}\,y^{-1}}$). These inter-annual variations are determined by climatic conditions that are themselves often linked to wind direction (North-East direction for dry and sunny weather, South-West direction for wet and cloudy weather, Granier et al., 2008). Consequently, in addition to the impact of the annual evolution in soil temperature and water content, the annual distribution of flux footprint combined with the spatial variation in F_S at Hesse is probably partly responsible for the annual R_{ECO} fluctuations, as already shown for mixed forest ecosystems (Aubinet et al., 2005; Göckede et al., 2008). The relatively large potential variations in the contribution of F_S to R_{ECO} when footprint is changing (possible F_S increases by over 50% if considering EC fluxes from one plot to another) may also be put forward as explanations for the large increases and decreases in R_{ECO} observed at Hesse at the half-hour time step, and which are visibly independent of climatic or edaphic conditions (Longdoz et al., 2008).

5. Conclusion

The present study revealed spatial variations in soil CO_2 efflux values in a quasi-homogeneous land cover type with vegetation surface characteristics classically considered as most suitable for EC measurements. Spatial variability at local plot scale was shown to be as large as or smaller than the spatial variability at whole-stand scale, thus justifying our use of a stratified sampling scheme with plot comparisons. We showed that the basal respiration rate was related to the bulk density and C/N ratio of the topsoil. Temporal integration to annual soil CO_2 efflux resulted in large spatial differences. The spatial heterogeneity of soil CO_2 efflux at stand scale, which is linked to the major contribution of soil CO_2 efflux to total ecosystem respiration and temporal variations of eddy covariance footprint, may be an important cause of the currently unexplained temporal fluctuations of measured total ecosystem respiration, and would thus be partly responsible for the difficulties involved in processing nighttime eddy covariance data. Combining the F_S map with footprint simulations may thus potentially help understand the causes of temporal variations in nighttime R_{ECO} measured at stand scale.

Acknowledgements

The authors thank François Willm, Bernard Clerc and François Gérémia (INRA Nancy, Nancy) for their valuable field assistance, M. Michel Yernaux (FUSAGx, Belgium) for kindly providing the temperature probes, and Yves Lefèvre (INRA Nancy, France) for providing precious knowledge on soil characteristics determination. We also thank Jacqueline Marchand (INRA Nancy, France) for the CHN analysis, and Patrick Gross and Pascal Courtois (INRA Nancy, France) for their continuous maintenance of the field instruments and assistance with collecting the micrometeorological data. We are grateful to Olivier Ryk for his valuable help in soil core sorting. Finally, the authors thank Kamel Soudani (University Paris-Sud, France) for valuable discussions on statistical analysis. This study was supported by the European project CarboEurope IP (FP6) and the French National Forestry Service (ONF). We also acknowledge the two anonymous reviewers for their constructive comments that improved the present manuscript.

References

Adachi, M., Bekku, Y.S., Konuma, A., Kadir, W.R., Okuda, T., Koizumi, H., 2005. Required sample size for estimating soil respiration rate in larges area of forests and of two types of plantation in Malaysia. Forest Ecol. Manage. 210, 455–456.

Aubinet, M., Berbigier, P., Bernhofer, C., Cescatti, A., Feigenwinter, C., Granier, A., Grunwald, T., Havrankova, K., Heinesch, B., Longdoz, B., Marcolla, B., Montagnani, L., Sedlak, P., 2005. Comparing CO_2 storage and advection conditions at night at different Carboeuroflux sites. Boundary-Layer Meteorol. 116, 63–94.

Bahn, M., Schmitt, M., Siegwolf, R., Richter, A., Brüggemann, N., 2009. Does photosynthesis affect grassland soil-respired CO_2 and its carbon isotope composition on a diurnal timescale? New Phytol. 182, 451–460, doi:10.1111/j.1469-8137.2008.02755.

Bahn, M., Reichstein, M., Davidson, E.A., Grünzweig, J., Jung, M., Carbone, M.S., Epron, D., Misson, L., Nouvellon, Y., Roupsard, O., Savage, K., Trumbore, S.E., Gimeno, C., Yuste, J.C., Tang, J., Vargas, R., Janssens, I.A., 2010. Soil respiration at mean annual temperature predicts annual total across vegetation types and biomes. Biogeosciences 7, 2147–2157.

Baldocchi, D., 2008. Breathing of the terrestrial biosphere: lessons learned from a global network of carbon dioxide flux measurement systems. Aust. J. Bot. 56, 1–26.

Beylich, A., Oberholzer, H.O., Schrader, S., Höper, H., Wilke, B.M., 2010. Evaluation of soil compaction effects on soil biota and soil biological processes in soils. Soil Tillage Res. 109, 133–143.

Boone, R.D., Nadelhoffer, K.J., Canary, J.D., Kaye, J.P., 1998. Roots exert a strong influence on the temperature sensitivity of soil respiration. Nature 396, 570–572.

Bouriaud, O., Soudani, K., Bréda, N., 2003. Leaf area index from litter collection: impact of specific leaf area variability within a beech stand. Can. J. Remote Sens. 29, 371–380.

Bréda, N., 1999. L'indice foliaire des couverts forestiers: mesure, variabilité et rôle fonctionnel. Rev. For. Fr. Li. 2, 135–150.

Chemidlin Prévost-Bouré, N., Soudani, K., Damesin, C., Berveiller, D., Lata, J.C., Dufrêne, E., 2010. Increase in aboveground fresh litter quantity over-stimulates soil respiration in a temperate deciduous forest. Appl. Soil Ecol. 46, 26–34.

Curiel Yuste, J., Janssens, I.A., Carrara, A., Meiresonne, L., Ceulemans, R., 2003. Interactive effects of temperature and precipitation on soil respiration in a temperate maritime pine forest. Tree Physiol. 23, 1263–1270.

Curiel Yuste, J., Nagy, M., Janssens, I.A., Carrara, A., Ceulemans, R., 2005. Soil respiration in a mixed temperate forest and its contribution to total ecosystem respiration. Tree Physiol. 25, 609–619.

d'Annunzio, M., Zeller, B., Nicolas, M., Dhote, J.F., Saint-Andre, L., 2008. Decomposition of European beech (*Fagus sylvatica*) litter: combining quality theory and ^{15}N labelling experiments. Soil Biol. Biochem. 40, 322–333.

Davidson, E.A., Belk, E., Boone, R.D., 1998. Soil water content and temperature as independent or confounded factors controlling soil respiration in a temperate mixed hardwood forest. Global Change Biol. 4, 217–227.

Davidson, E.A., Janssens, I.A., Luo, Y., 2006. On the variability of respiration in terrestrial ecosystems: moving beyond Q_{10}. Global Change Biol. 12, 154–164.

Desai, A., Richardson, A.D., Moffat, A.M., Kattge, J., Hollinger, D.Y., Barr, A., Falge, E., Noormets, A., Papale, D., Reichstein, M., Stauch, V.J., 2008. Cross-site evaluation of eddy covariance GPP and RE decomposition techniques. Agric. Forest Meterol. 148, 821–838.

Epron, D., Farque, L., Lucot, E., Badot, P.M., 1999. Soil CO_2 efflux in a beech forest: dependence on soil temperature and soil water content. Ann. Forest Sci. 56, 221–226.

Epron, D., Le Dantec, V., Dufrêne, E., Granier, A., 2001. Seasonal dynamics of soil carbon dioxide efflux and simulated rhizosphere respiration in a beech forest. Tree Physiol. 21, 145–152.

Epron, D., Ngao, J., Granier, A., 2004a. Interannual variation of soil respiration in a beech forest ecosystem over a six-year study. Ann. Forest Sci. 61, 499–505.

Epron, D., Nouvellon, Y., Roupsard, O., Mouvondy, W., Mabiala, A., Saint-Andre, L., Joffre, R., Jourdan, C., Bonnefond, J.M., Berbigier, P., Hamel, O., 2004b. Spatial and temporal variations of soil respiration in a Eucalyptus plantation in Congo. Forest Ecol. Manage. 204, 149–160.

Epron, D., Bosc, A., Bonal, D., Freycon, V., 2006. Spatial variation of soil respiration across a topographic gradient in a tropical rain forest in French Guiana. J. Trop. Ecol. 22, 565–574.

Franzluebbers, A.J., 1999. Microbial activity in response to water-filled pore space of variably eroded southern Piedmont soils. Appl. Soil Ecol. 11, 91–101, doi:10.1016/S0929-1393(98)00128-0.

Göckede, M., Foken, T., Aubinet, M., Aurela, M., Banza, J., Bernhofer, C., Brunet, Y., Carrara, A., Clement, R., Dellwik, E., Elbers, J., Eugster, W., Fuhrer, J., Granier, A., Grünwald, T., Heinesch, B., Janssens, I.A., Jarosz, N., Knohl, A., Koeble, R., Laurila, T., Longdoz, B., Loustau, D., Manca, G., Marek, M., Markkanen, T., Mateus, J., Matteucci, G., Mauder, M., Migliavacca, M., Minerbi, S., Moncrieff, J., Montagnani, L., Moors, E., Ourcival, J.M., Papale, D., Pereira, J., Pilegaard, K., Pita, G., Rambal, S., Rebmann, C., Rotenberg, E., Sanz, M.J., Sedlak, P., Seufert, G., Siebicke, L., Soussana, J.F., Valentini, R., Vesala, T., Verbeeck, H., Yakir, D., 2008. Quality control of CarboEurope flux data – part 1: coupling footprint analyses with flux data quality assessment to evaluate sites in forest ecosystems. Biogeosciences 5, 433–450.

Granier, A., Breda, N., Biron, P., Villette, S., 1999. A lumped water balance model to evaluate duration and intensity of drought constraints in forest stands. Ecol. Model. 116, 269–283.

Granier, A., Ceschia, E., Damesin, C., Dufrene, E., Epron, D., Gross, P., Lebaude, S., Le Dantec, V., Le Goff, N., Lemoine, L., Lucot, E., Ottorini, J.M., Pontailler, J.Y., Saugier, B., 2000. The carbon balance of a young Beech forest. Funct. Ecol. 14, 312–325.

Granier, A., Reichstein, M., Breda, N., Janssens, I.A., Falge, E., Ciais, P., Grünwald, T., Aubinet, M., Berbigier, P., Bernhofer, C., Buchmann, N., Facini, O., Grassi, G., Heinesch, B., Ilvesniemi, H., Keronen, P., Knohl, A., Kostner, B., Lagergren, F., Lindroth, A., Longdoz, B., Loustau, D., Mateus, J., Montagnani, L., Nys, C., Moors, E., Papale, D., Peiffer, M., Pilegaard, K., Pita, G., Pumpanen, J., Rambal, S., Rebmann, C., Rodrigues, A., Seufert, G., Tenhunen, J., Vesala, T., Wang, Q., 2007. Evidence for soil water control on carbon and water dynamics in European forests during the extremely dry year: 2003. Agric. Forest Meterol. 143, 123–145.

Granier, A., Bréda, N., Longdoz, B., Gross, P., Ngao, J., 2008. Ten years of fluxes and stand growth in a young beech forest at Hesse, North-eastern France. Ann. Forest Sci. 64, 704–716.

Högberg, P., Nordgren, A., Buchmann, N., Taylor, A.F.S., Ekblad, A., Hogberg, M.N., Nyberg, G., Ottoson-Löfvenius, M., Read, D.J., 2001. Large-scale forest girdling shows that current photosynthesis drives soil respiration. Nature 411, 789–792.

Janssens, I.A., Kowalski, A.S., Ceulemans, R., 2001a. Forest floor CO_2 fluxes estimated by eddy covariance and chamber-based model. Agric. Forest Meterol. 106, 61–69.

Janssens, I.A., Lankreijer, H., Matteucci, G., Kowalski, A.S., Buchmann, N., Epron, D., Pilegaard, K., Kutsch, W., Longdoz, B., Grünwald, T., Montagnani, L., Dore, S., Rebmann, C., Moors, E.J., Grelle, A., Rannik, Ü., Morgenstern, K., Oltchev, S., Clement, R., Gudmundson, J., Minerbi, S., Berbigier, P., Ibrom, A., Moncrieff, J.B., Aubinet, M., Bernhofer, C., Jensen, N.O., Vesala, T., Granier, A., Schulze, E.D., Lindroth, A., Dolman, A.J., Jarvis, P.G., Ceulemans, R., Valentini, R., 2001b. Productivity overshadows temperature in determining soil and ecosystem respiration across European forests. Global Change Biol. 7, 269–278.

Janssens, I.A., Dore, S., Epron, D., Lankreijer, H., Buchmann, N., Longdoz, B., Brossaud, J., Montagnani, L., 2003. Climatic influences on seasonal and spatial differences in soil CO_2 efflux. Fluxes of Carbon, Water and Energy of European Forests, 163. Springer-Verlag, Berlin, pp. 233–253.

Janssens, I.A., Pilegaard, K., 2003. Large seasonal changes in $Q(10)$ of soil respiration in a beech forest. Global Change Biol. 9, 911–918.

Khomik, M., Arain, M.A., McCaughey, J.H., 2006. Temporal and spatial variability of soil respiration in a boreal mixedwood forest. Agric. Forest Meterol. 140, 244–256.

Khomik, M., Arain, M.A., Brodeur, J.J., Peichl, M., Restrepo-Coupe, N., McLaren, J.D., 2010. Relative contributions of soil, foliar, and woody tissue respiration to total ecosystem respiration in four pine forests of different ages. J. Geophys. Res. 115, G03024.

Knohl, A., Søe, A.R.B., Kutsch, W.L., Göckede, M., Buchmann, N., 2008. Representative estimates of soil and ecosystem respiration in an old beech forest. Plant Soil 302, 189–202.

Kosugi, Y., Mitani, T., Itoh, M., Noguchi, S., Tani, M., Matsuo, N., Takanashi, S., Ohkubo, S., Nik, A.R., 2007. Spatial and temporal variation in soil respiration in a Southeast Asian tropical rainforest. Agric. Forest Meterol. 147, 35–47.

Lavigne, M.B., Foster, R.J., Goodine, G., 2004. Seasonal and annual changes in soil respiration in relation to soil temperature, water potential and trenching. Tree Physiol. 24, 415–424.

Leuschner, C., Voß, S., Foetzki, A., Clases, Y., 2006. Variation in leaf area index and stand leaf mass of European beech across gradients of soil acidity and precipitation. Plant Ecol. 182, 247–258.

Longdoz, B., Yernaux, M., Aubinet, M., 2000. Soil CO_2 efflux measurements in a mixed forest: impact of chamber disturbances, spatial variability and seasonal evolution. Global Change Biol. 6, 907–917.

Longdoz, B., Gross, P., Granier, A., 2008. Multiple quality tests for analysing CO_2 fluxes in a beech temperate forest. Biogeosciences 5, 719–729.

Luyssaert, S., Reichstein, M., Schulze, E.D., Janssens, I.A., Law, B.E., Papale, D., Dragoni, D., Goulden, M.L., Granier, A., Kutsch, W.L., Linder, S., Matteucci, G., Moors, E., Munger, J.W., Pilegaard, K., Saunders, M., Falge, E.M., 2009. Toward a consistency cross-check of eddy covariance flux-based and biometric estimates of ecosystem carbon balance. Global Biogeochem. Cycles 23, GB3009.

Mariani, L., Chang, S.X., Kabzems, R., 2006. Effects of tree harvesting, forest floor removal, and compaction on soil microbial biomass, microbial respiration, and N availability in a boreal aspen forest in British Columbia. Soil Biol. Biochem. 38, 1734–1744.

Marron, N., Plain, C., Longdoz, B., Epron, D., 2009. Seasonal and daily time course of the 13C composition in soil CO_2 efflux recorded with a tunable diode laser spectrophotometer (TDLS). Plant Soil 318, 137–151.

Melillo, J.M., Aber, J.D., Muratore, J.F., 1982. Nitrogen and lignin control of hardwood leaf litter decomposition dynamics. Ecology 63, 621–626.

Ngao, J., Perrin, D., Vincent, G., Epron, D., Le Dantec, V., Soudani, K., Aubinet, M., Granier, A., Willm, F., Longdoz, B., 2006. Cross-calibration functions for soil CO_2 efflux measurement systems. Ann. Forest Sci. 63, 477–484.

Ngao, J., Longdoz, B., Granier, A., Epron, D., 2007. Separating autotrophic and heterotrophic respiration in two young beech stands: impact of corrections for root decomposition in trenched plots. Plant Soil 301, 99–110.

Norby, R.J., Cotrufo, M.F., Ineson, P., O'Neill, E.G., Canadell, J.G., 2001. Elevated CO_2, litter chemistry, and decomposition: a synthesis. Oecologia 127, 153–165.

Ohashi, M., Gyokusen, K., 2007. Temporal change in spatial variability of soil respiration on a slope of Japanese cedar (*Cryptomeria japonica* D. Don) forest. Soil Biol. Biochem. 39, 1130–1138.

Ohkubo, S., Kosugi, Y., Takanashi, S., Mitani, T., Tani, M., 2007. Comparison of the eddy covariance and automated closed chamber methods for evaluating nocturnal CO_2 exchange in a Japanese cypress forest. Agric. Forest Meterol. 142, 50–65.

Quentin, C., Bigorre, F., Tessier, D., Granier, A., Bréda, N., 2001. Etude des sols de la Forêt de Hesse (Lorraine). Contribution à l'étude du bilan hydrique. Etud. Gestion Sols 8, 279–292.

Rebmann, C., Göckede, M., Foken, T., Aubinet, M., Aurela, M., Berbigier, P., Bernhofer, C., Buchmann, N., Carrara, A., Cescatti, A., Ceulemans, R., Clement, R., Elbers, J.A., Granier, A., Grünwald, T., Guyon, D., Havránkova, K., Heinesch, B., Knohl, A., Laurila, T., Longdoz, B., Marcolla, B., Markkanen, T., Miglietta, F., Moncrieff, J.B., Montagnani, L., Moors, E., Nardino, M., Ourcival, J.M., Rambal, S., Rannik, Ü., Rotenberg, E., Sedlak, P., Unterhuber, G., Vesala, T., Yakir, D., 2005. Quality analysis applied on eddy covariance measurements at complex forest sites using footprint modelling. Theor. Appl. Climatol. 80, 121–141.

Reichstein, M., Tenhunen, J., Roupsard, O., Ourcival, J.M., Rambal, S., Dore, S., Valentini, R., 2002. Ecosystem respiration in two Mediterranean evergreen Holm Oak forests: drought effects and decomposition dynamics. Funct. Ecol. 16, 27–39.

Reichstein, M., Rey, A., Freibauer, A., Tenhunen, J., Valentini, R., Banza, J., Casals, P., Cheng, Y., Grünzweig, J.M., Irvine, J., Joffre, R., Law, B.E., Loustau, D., Miglietta, F., Oechel, W., Ourcival, J.M., Pereira, J.S., Peressotti, A., Ponti, F., Qi, Y., Rambal, S., Rayment, M., Romanya, J., Rossi, F., Tedeschi, V., Tirone, G., Xu, M., Yakir, D., 2003. Modeling temporal and large-scale spatial variability of soil respiration from soil water availability, temperature and vegetation productivity indices. Global Biogeochem. Cycles 17, 1104.

Rey, A., Pegoraro, E., Tedeschi, V., Deparri, I., Jarvis, P.G., Valentini, R., 2002. Annual variation in soil respiration and its components in a coppice oak forest in Central Italy. Global Change Biol. 8, 851–866.

Rodeghiero, M., Cescatti, A., 2008. Spatial variability and optimal sampling strategy of soil respiration. Forest Ecol. Manage. 255, 106–112.

Ruehr, N.K., Buchmann, N., 2010. Soil respiration fluxes in a temperate mixed forest: seasonality and temperature sensitivities differ among microbial and root-rhizosphere respiration. Tree Physiol. 30, 165–176.

Saiz, G., Green, C., Butterbach-Bahl, K., Kiese, R., Avitabile, V., Farrell, E.P., 2006. Seasonal and spatial variability of soil respiration in four Sitka spruce stands. Plant Soil 287, 161–176.

Sampson, D.A., Janssens, I.A., Curiel Yuste, J., Ceulemans, R., 2007. Basal rates of soil respiration are correlated with photosynthesis in a mixed temperate forest. Global Change Biol. 13, 2008–2017.

Savage, K.E., Davidson, E.A., 2003. A comparison of manual and automated systems for soil CO_2 flux measurements: trade-offs between spatial and temporal resolution. J. Exp. Bot. 54, 891–899.

Søe, A.R.B., Buchmann, N., 2005. Spatial and temporal variations in soil respiration in relation to stand structure and soil parameters in an unmanaged beech forest. Tree Physiol. 25, 1427–1436.

Subke, J.A., Reichstein, M., Tenhunen, J.D., 2003. Explaining temporal variation in soil CO_2 efflux in a mature spruce forest in Southern Germany. Soil Biol. Biochem. 35, 1467–1483.

Subke, J.A., Inglima, I., Cotrufo, M.F., 2006. Trends and methodological impacts in soil CO_2 efflux partitioning: a meta-analytical review. Global Change Biol. 12, 921–943.

Tang, J., Baldocchi, D., 2005. Spatial-temporal variation in soil respiration in an oak-grass savanna ecosystem in California and its partitioning into autotrophic and heterotrophic components. Biogeochemistry 73, 183–207.

Taylor, B.R., Parkinson, D., Parsons, W.F.J., 1989. Nitrogen and lignin content as predictors of litter decay rates. A microcosm test. Ecology 70, 97–104.

Valentini, R., Matteucci, G., Dolman, A.J., Schulze, E.D., Rebmann, C., Moors, E.J., Granier, A., Gross, P., Jensen, N.O., Pilegaard, K., Lindroth, A., Grelle, A., Bernhofer, C., Grünwald, T., Aubinet, M., Ceulemans, R., Kowalski, A.S., Vesala, T., Rannik, Ü., Berbigier, P., Lousteau, D., Guomundsson, J., Thorgeirsson, H., Ibrom, A., Morgenstern, K., Clement, R., Moncrieff, J.B., Montagnani, L., Minerbi, S., Jarvis, P.G., 2000. Respiration as the main determinant of carbon balance in European forests. Nature 404, 861–864.

Van Gorsel, E., Delpierre, N., Leuning, R., Black, A., Munger, J.W., Wofsy, S., Aubinet, M., Feigenwinter, C., Beringer, J., Bonal, D., Chen, B., Chen, J., Clement, R., Davis, K.J., Desai, A.R., Dragoni, D., Etzold, S., Grünwald, T., Gu, L., Heinesch, B., Hutyra, L.R., Jans, W.W.P., Kutsch, W., Law, B.E., Leclerc, M.Y., Mammarella, I., Montagnani, L., Noormets, A., Rebmann, C., Wharton, S., 2009. Estimating nocturnal ecosystem respiration from the vertical turbulent flux and change in storage of CO_2. Agric. Forest Meterol. 149, 1919–1930.

Vesterdal, L., Schmidt, I.K., Callesen, I., Nilsson, L.O., Gundersen, P., 2008. Carbon and nitrogen in forest floor and mineral soil under six common European tree species. Forest Ecol. Manage. 255, 35–48.

Vincent, G., Shahriari, A.R., Lucot, E., Badot, P.M., Epron, D., 2006. Spatial and seasonal variations in soil respiration in a temperate deciduous forest with fluctuating water table. Soil Biol. Biochem. 38, 2527–2535.

Williams, B., 1993. Biostatistics, Concepts and Applications for Biologists. Chapman & Hall, London, 201 pp.

Xu, M., Qi, Y., 2001. Spatial and seasonal variation of Q_{10} determined by soil respiration measurements at a Sierra Nevadan forest. Global Biogeochem. Cycles 15, 687–696.

Yim, M.H., Joo, S.J., Shutou, K., Nakane, K., 2003. Spatial variability of soil respiration in a larch plantation: estimation of the number of sampling point required. Forest Ecol. Manage. 175, 585–588.